Support Information

Strain engineering in oxygen reduction reaction and oxygen evolution reaction catalyzed by Pt-doped Ti_2CF_2

Ninggui Ma,[a] *Na Li,* [a] *Tairan Wang,* [a] *Xinyao Ma* [a] *and Jun Fan* [a, b, c,]*

[a] Department of Materials Science and Engineering, City University of Hong Kong, Hong Kong, China

[b] Department of Mechanical Engineering, City University of Hong Kong, Hong Kong, China

[c] Center for Advance Nuclear Safety and Sustainable Department, City University of Hong Kong, China

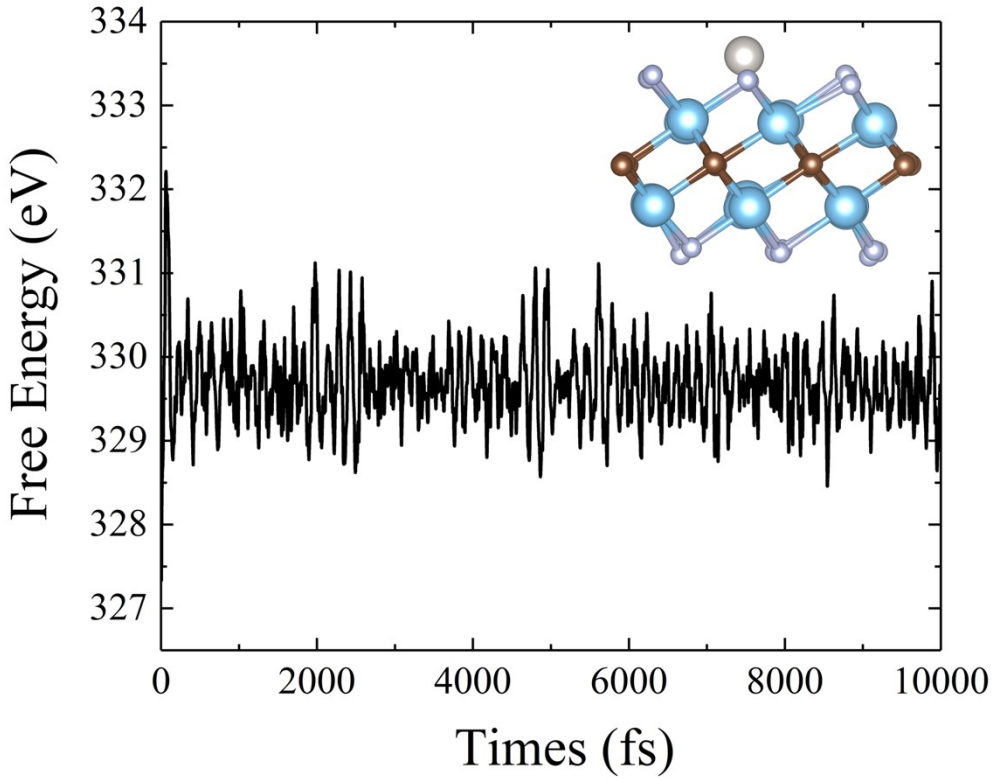

Fig. S1 Variation of the free energy and the structure in the AIMD simulations at 500 K during the time scale of 10 ps for Pt-V_F-Ti_2CF_2.

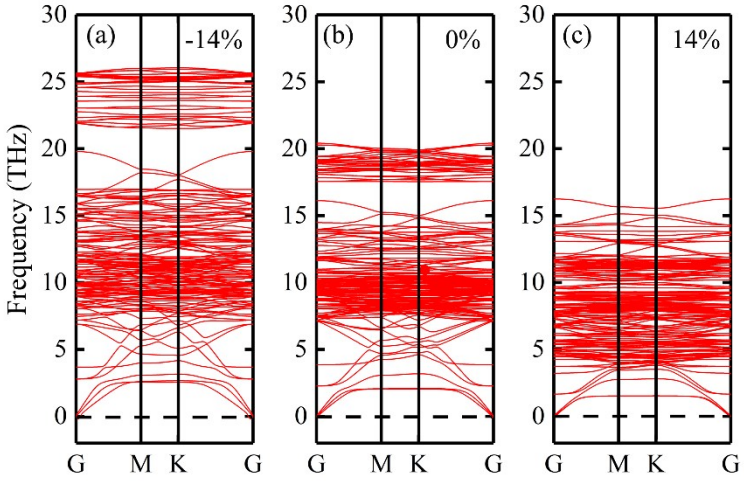

Fig. S2 (a), (b) and (c) the Phonon dispersion for Pt-V_F-Ti_2CF_2 under -14%, 0% and 14% biaxial strain, respectively.

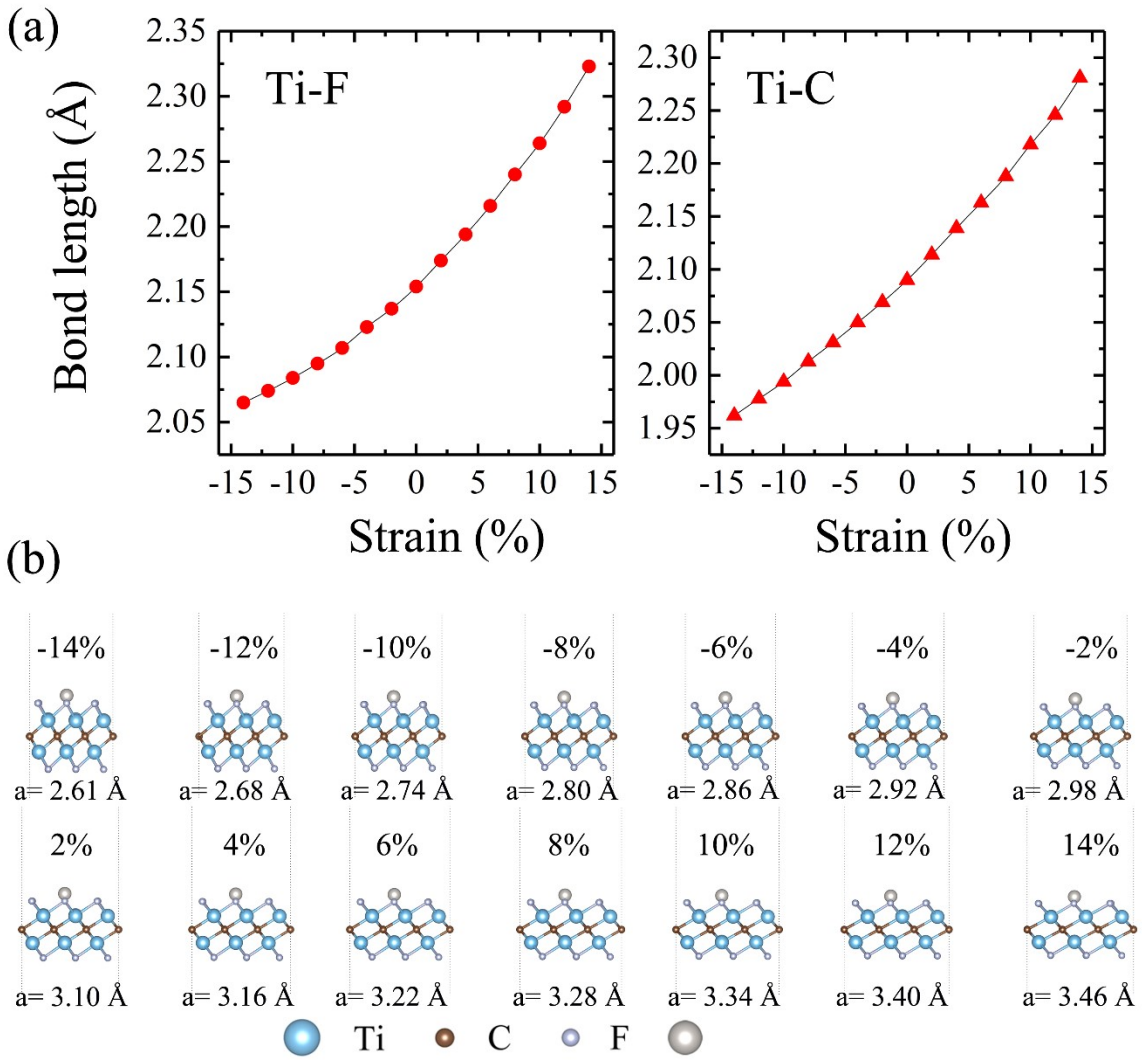

Fig. S3 (a) Strain dependence of bond lengths for Ti-F and Ti-C in Pt-V_F-Ti_2CF_2. (b) The structure of Pt-V_F-Ti_2CF_2 under the different biaxial strain from -14% to 14%. The blue, lavender, brown and gray balls represent Ti, F, C and Pt atoms, respectively.

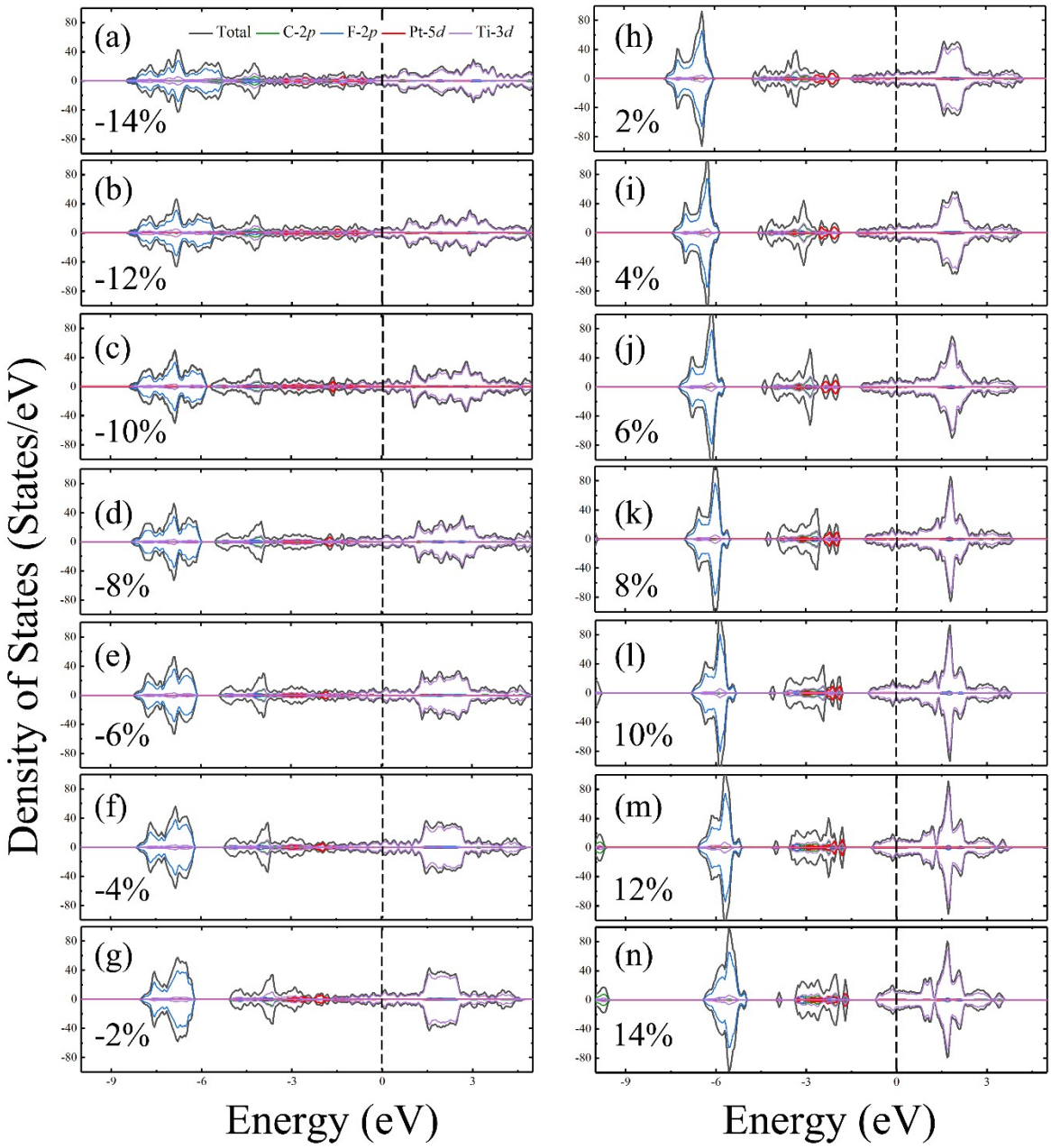

Fig. S4 The DOS and PDOS of Pt-V_F-Ti_2CF_2 under the different biaxial strain from -14% to 14%. The Fermi level is set to zero.

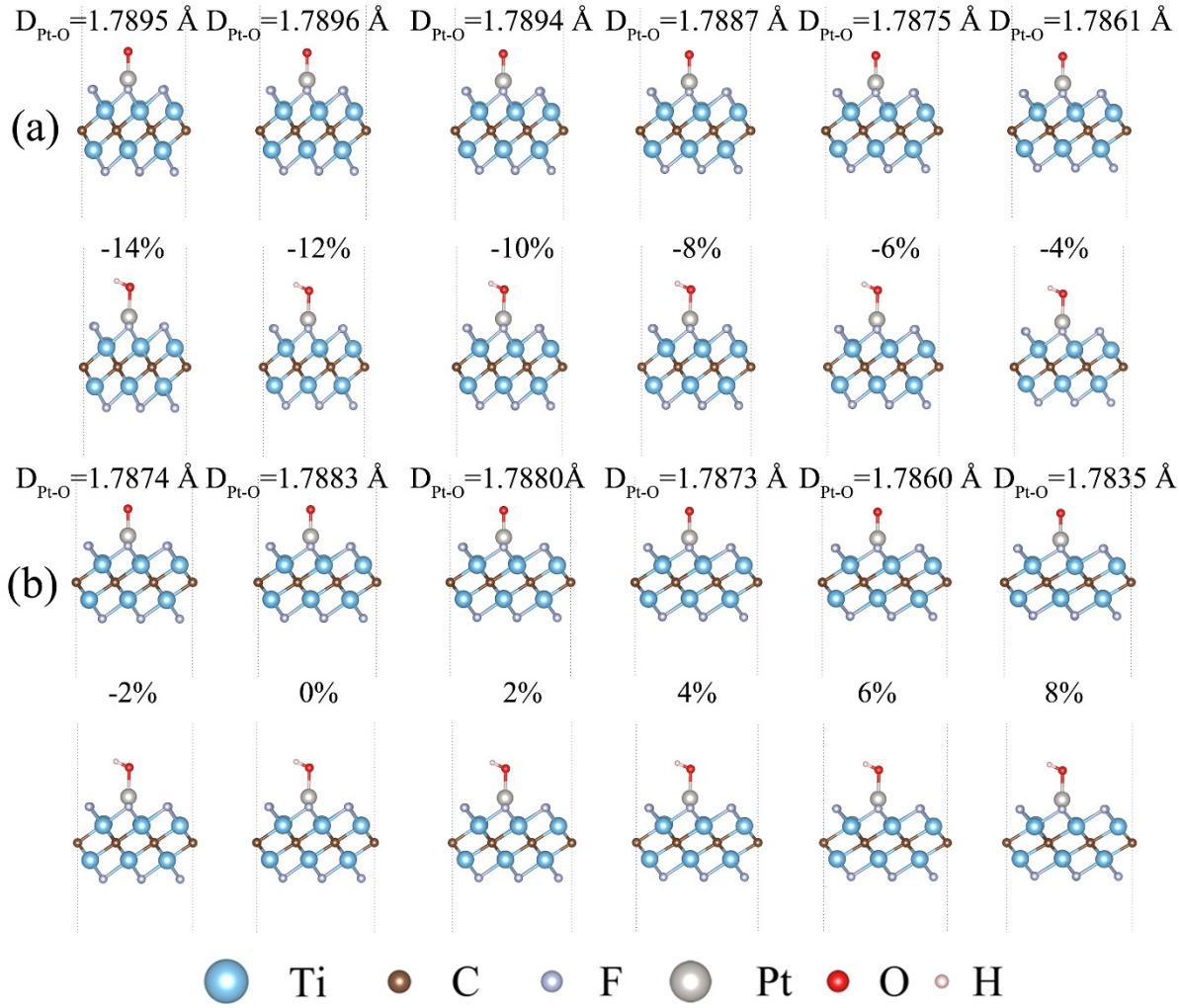

Fig. S5 The structure of *O and *OH under the different biaxial strain from -14% to 8%. The blue, brown, lavender, gray, red and lavenderblush balls represent Ti, C, F, Pt, O and H atoms, respectively.

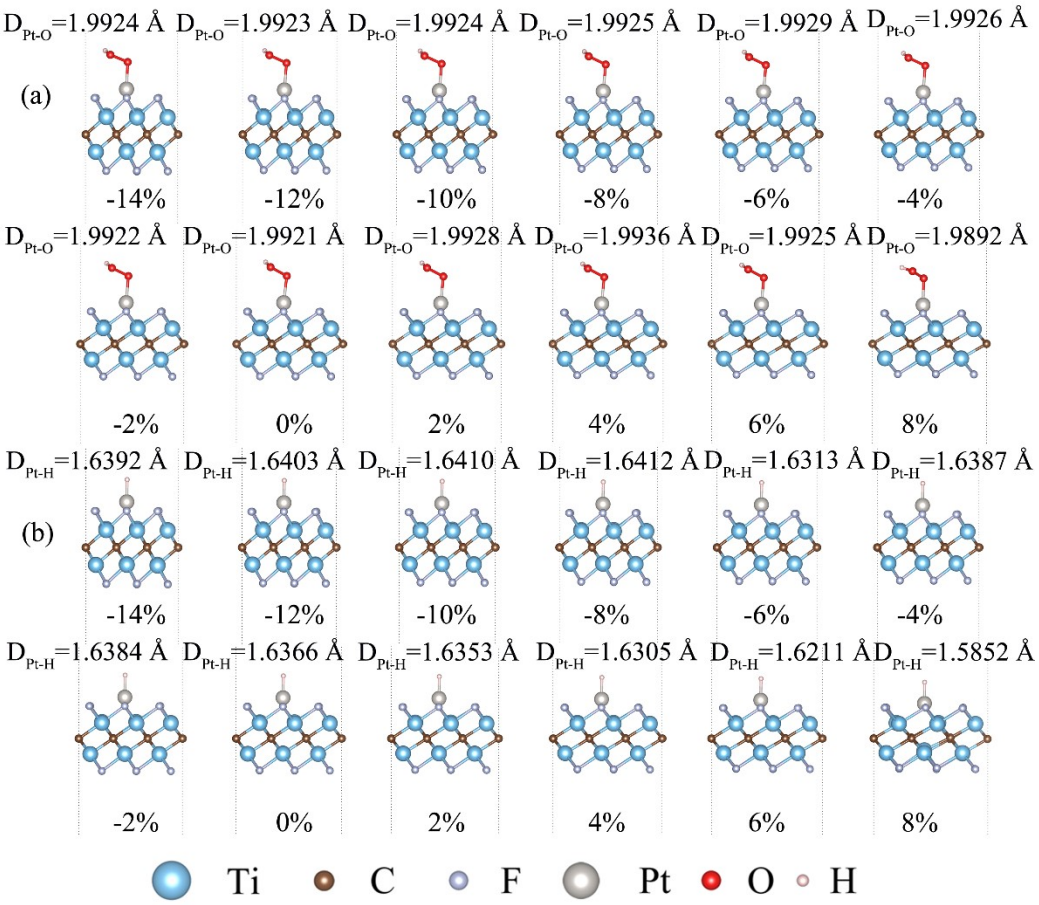

Fig. S6 The structure of *OOH and *H under the different biaxial strain from -14% to 8%. The blue, brown, lavender, gray, red and lavenderblush balls represent Ti, C, F, Pt, O and H atoms, respectively.

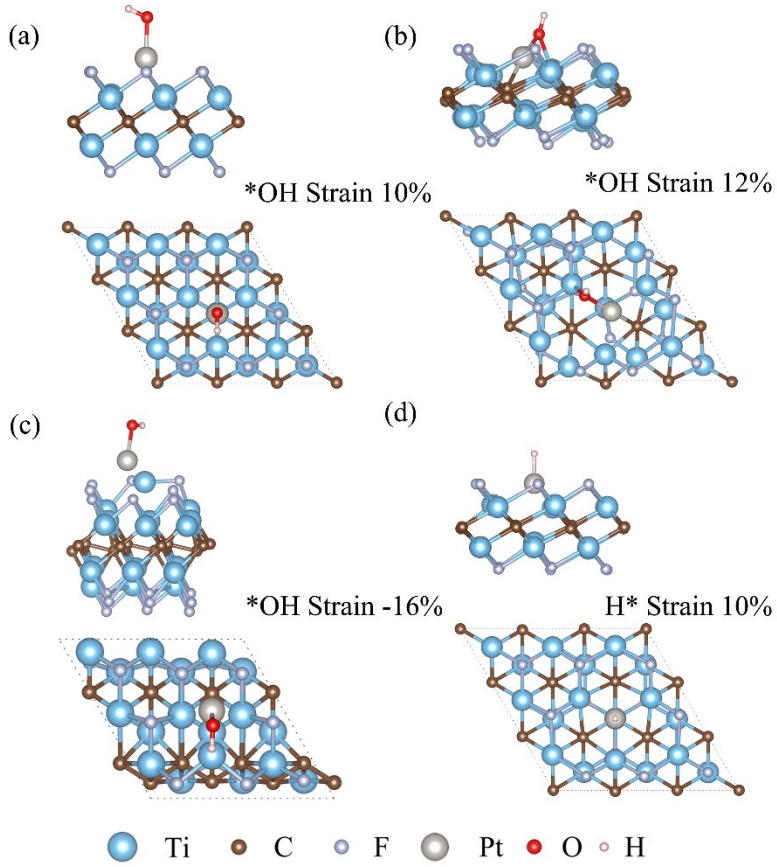

Fig. S7 (a) and (b) The structure of *OH under the 10% and 12% tensile strain. (c) The structure of *OH under the -16&compressive strain. (d) The structure of *H under 10% tensile strain. The blue, brown, lavender, gray, red and lavenderblush balls represent Ti, C, F, Pt, O and H atoms, respectively.

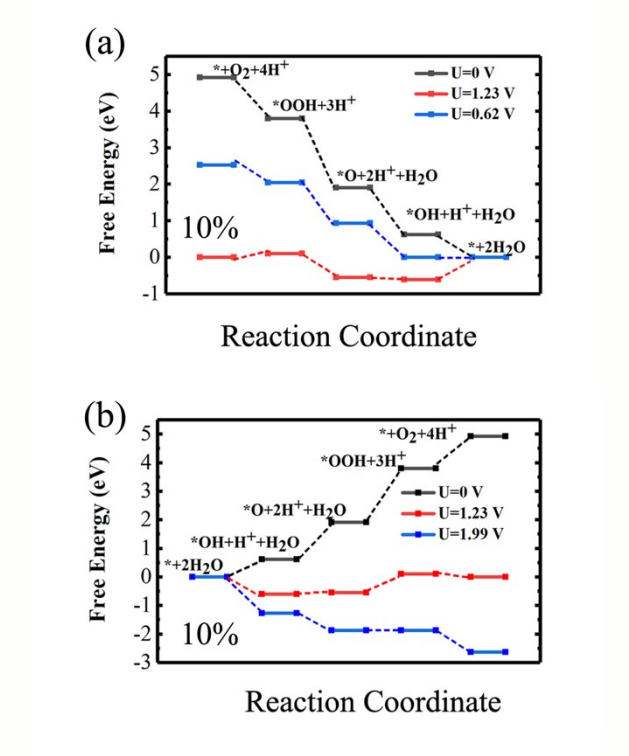

Fig. S8 The Gibbs free energy change diagram of catalytic reaction for ORR (a) and OER(b) on Pt-V_F-Ti_2CF_2 under 10% strain.

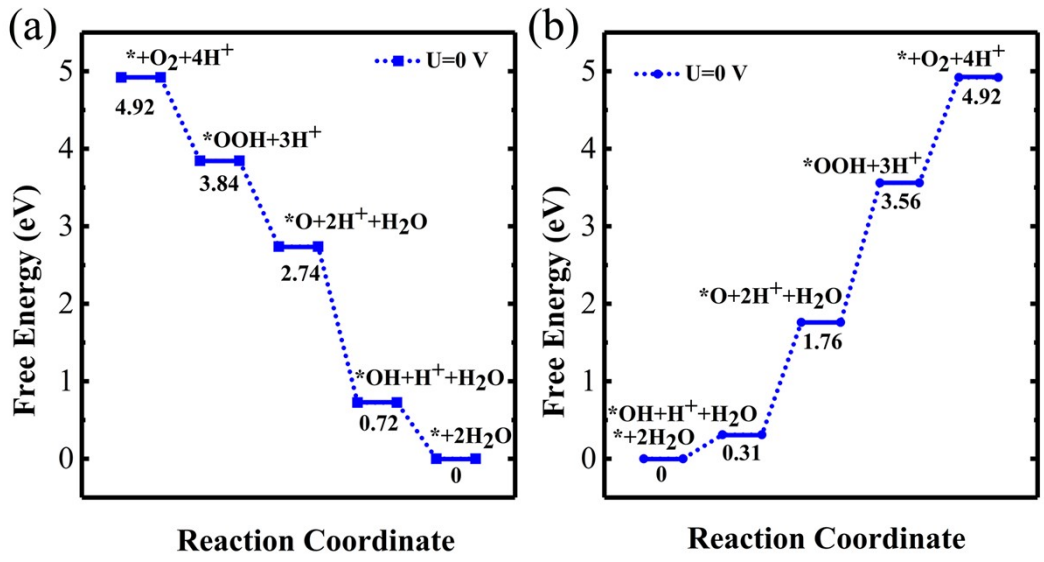

Fig. S9 The Gibbs free energy change diagram of catalytic reaction for ORR (a) and OER(b) on Pt-V_F-Ti_2CF_2 with the considering of the salvation effect under -14% and 4% strain, respectively.

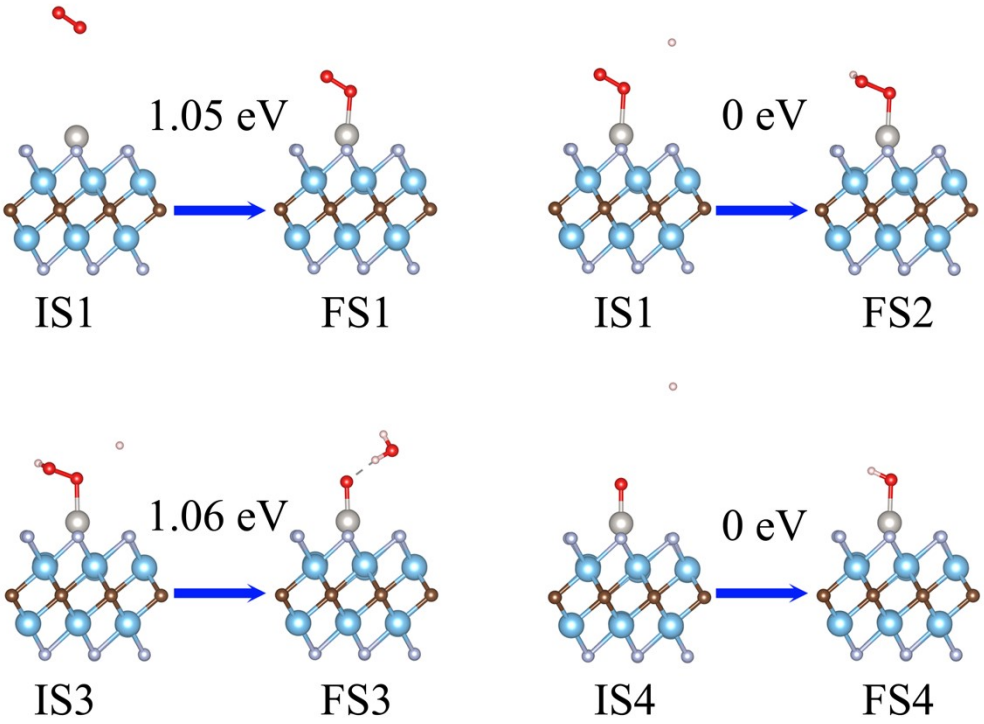

Fig. S10 Schematic diagram of the kinetic reaction process for the ORR, Pt-V_F-Ti_2CF_2 under -14% strain. IS and FS represent the initial site and final site, respectively.

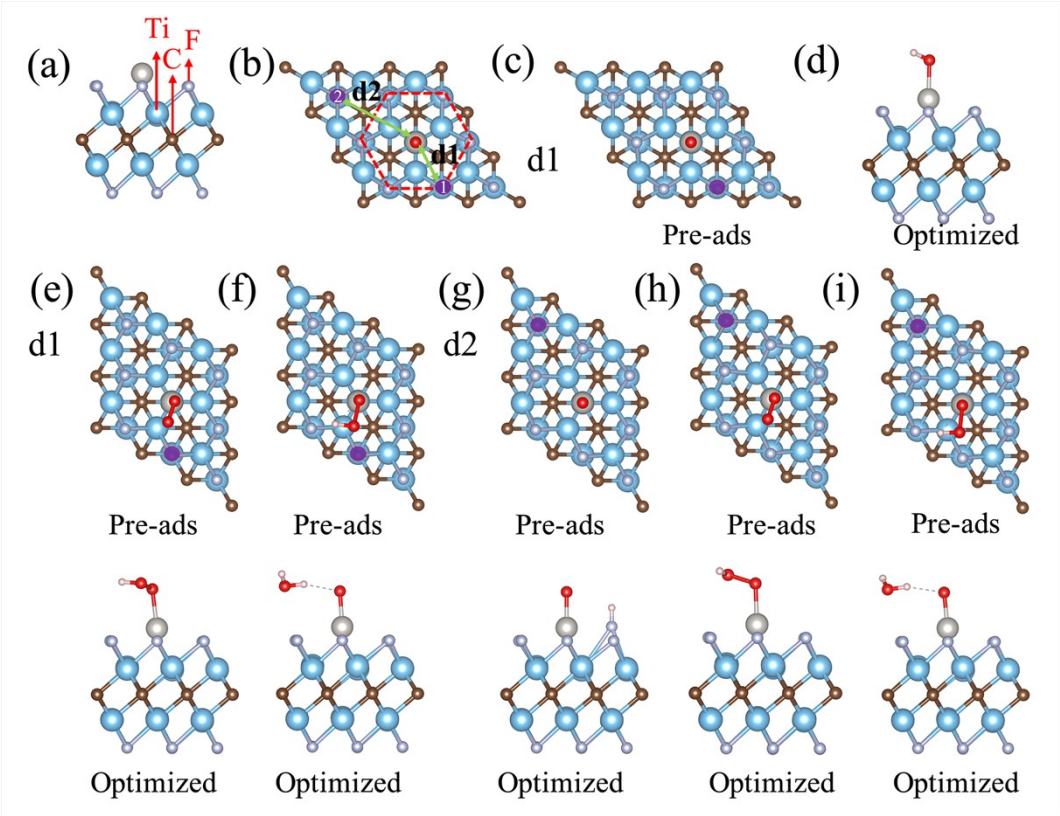

Fig. S11 (a) The sites of the H atom adsorption on the Pt-V_F-Ti_2CF_2. (b) The sites of the H atom adsorption on Pt-V_F-Ti_2CF_2 with catalytic intermediates. The pre-adsorption model of H on *O with the d1 distributed (c) and optimized model (d). The pre-adsorption model and optimized model of H atom adsorption on *O_2 (e) and *OOH (f) with the d1 distributed. The pre-adsorption model and optimized model of H atom adsorption on *O (g), *O_2 (h) and *OOH (i) with the d2 distributed. The purple circle represents the adsorption position of the H atom.

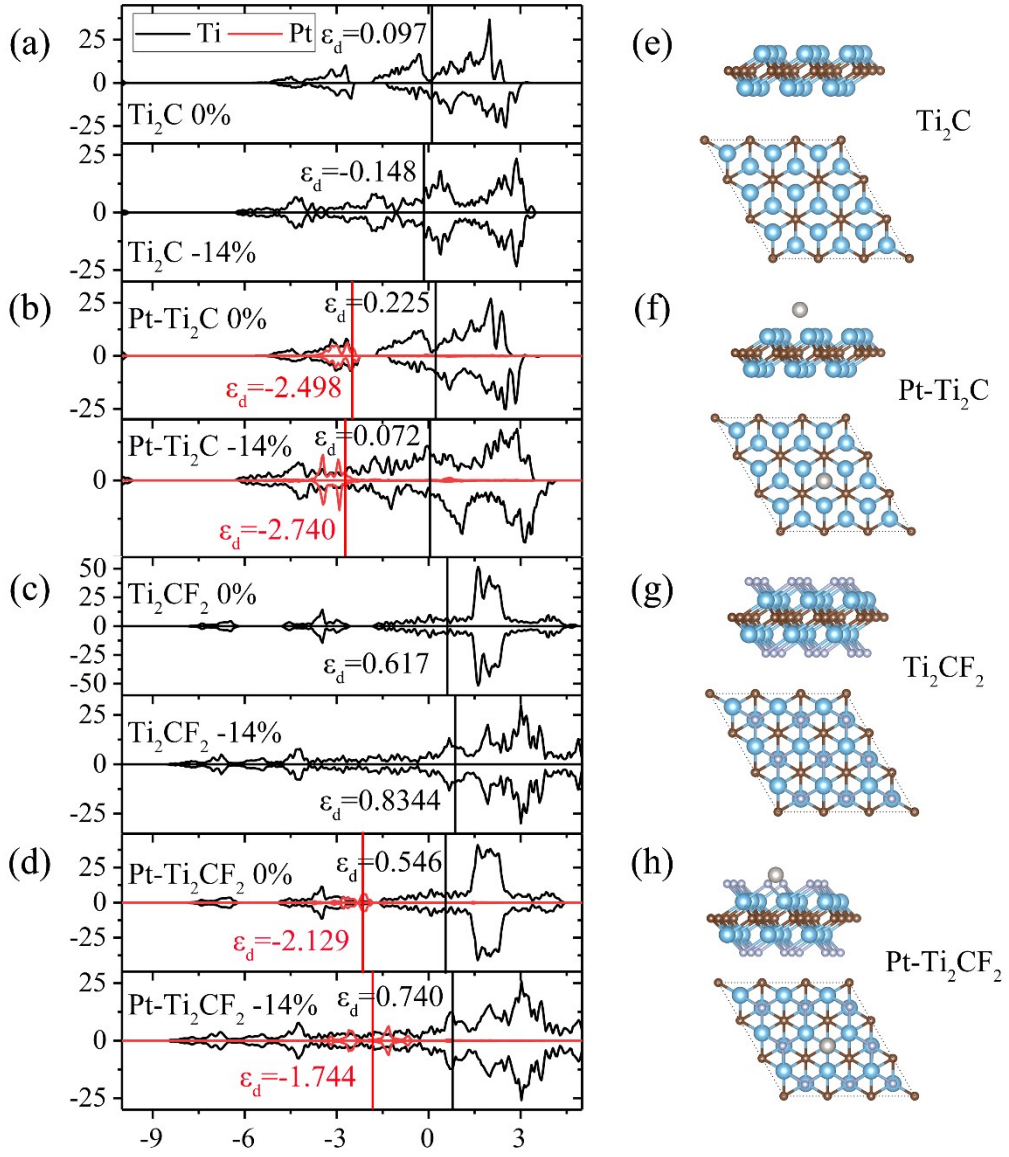

Fig. S12 (a) The DOS of Ti in Ti_2C under the biaxial strain 0 and -14%. (b) The DOS of Ti and Pt in Pt-Ti_2C under the biaxial strain 0 and -14%. (c) The DOS of Ti in Ti_2CF_2 under the biaxial strain 0 and -14%. (d) The DOS of Ti and Pt in Pt-Ti_2CF_2 under the biaxial strain 0 and -14%. (e-f) The side and top view of Ti_2C, Pt-Ti_2C, Ti_2CF_2 and Pt-V_F-Ti_2CF_2. The Fermi level is set to zero.

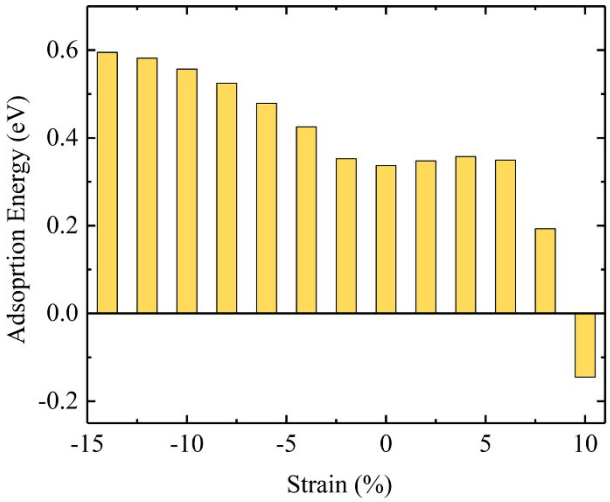

Fig. S13 The adsorption energy of H atom on Pt-V_F-Ti_2CF_2 under the different biaxial strain from -14% to 10%.

Table S1 The Gibbs free energy of each step on the Pt-V_F-Ti_2CF_2 toward ORR, OER and HER

Strains (%)	G_{*OH} (eV)	G_{*O} (eV)	G_{*OOH} (eV)	G_{*H} (eV)
-14	0.78	2.8	3.96	0.84
-12	0.75	2.74	3.95	0.82
-10	0.70	2.67	3.96	0.80
-8	0.67	2.59	3.89	0.76
-6	0.64	2.50	3.88	0.72
-4	0.58	2.37	3.83	0.67
-2	0.52	2.23	3.76	0.59
0	0.50	2.19	3.76	0.58
2	0.52	2.19	3.79	0.59
4	0.54	2.18	3.85	0.60
6	0.58	2.18	3.87	0.59
8	0.60	2.13	3.84	0.43
10	0.62	1.91	3.80	0.10

Table S2 The energy corrections ($\Delta ZPE - T\Delta S$) in ORR and OER on all the catalysts

Strains (%)	*OH (eV)	*O (eV)	*OOH (eV)
-14	0.26	0.01	0.32
-12	0.26	0.01	0.31
-10	0.25	0.01	0.34
-8	0.26	0.01	0.29
-6	0.26	0.021	0.31
-4	0.25	0.02	0.30
-2	0.27	0.02	0.30
0	0.26	0.02	0.30
2	0.25	0.01	0.31
4	0.25	0.01	0.33
6	0.25	0.02	0.33
8	0.25	0.01	0.29
10	0.25	0.02	0.32

Table S3 The solvation energy corrections (ΔSol) and the free energy after considering the solvation effect on Pt-V_F-Ti_2CF_2, under -14% and 0% strain.

strain	ΔSol (eV)			ΔG_{sol} (eV)		
	*O	*OH	*OOH	*O	*OH	*OOH
-14%	-0.15	-0.15	-0.21	0.72	2.74	3.84
4%	-0.64	-0.45	-0.51	0.31	1.76	3.56

Table S4 The bond length of Pt-O in *OH for Pt-V_F-Ti_2CF_{22} under the different biaxial strain from -14% to 10% and the adsorption energy of OH on the Pt-V_F-Ti_2CF_2 under the different biaxial strain from -14% to 10%

Strains (%)	Pt-O (Å)	E_{OH} (eV)
-14	1.956	0.50
-12	1.957	0.47
-10	1.957	0.43
-8	1.958	0.39
-6	1.959	0.36
-4	1.960	0.30
-2	1.961	0.23
0	1.962	0.22
2	1.963	0.25
4	1.963	0.28
6	1.962	0.30
8	1.962	0.33
10	1.960	0.35

Table S5 Conducted the Bader charge analysis in ORR and OER for all catalytic intermediates. For the *OOH, the O1 is bind with Pt atoms

Strains (%)	Pt-V_F-Ti_2CF_2 (e)	*OH (e)		*O (e)	*OOH(e)		
	Pt	O	H	O	O1	O2	H
-14	10.02	6.75	0.74	6.70	6.46	5.98	0.93
-12	10.04	6.78	0.74	6.61	6.52	6.32	0.65
-10	10.25	6.70	0.81	6.60	6.69	5.43	1.14
-8	10.51	6.84	0.68	6.71	6.68	5.84	1.02
-6	10.11	6.87	0.62	6.71	6.47	6.31	0.67
-4	10.21	6.88	0.57	6.66	6.50	6.38	0.60
-2	10.31	6.86	0.68	6.73	6.47	6.17	0.81
0	10.35	6.89	0.68	6.60	6.57	6.15	0.79
2	10.26	6.86	0.66	6.65	6.54	6.23	0.74
4	10.35	6.89	0.62	6.68	6.53	6.23	0.67
6	10.34	6.88	0.60	6.65	6.53	6.38	0.60
8	10.36	6.97	0.53	6.68	6.41	6.25	0.73
10	10.47	6.94	0.59	6.70	6.46	6.47	0.57

Calculation details

In this work, the overall catalytic reactions are carried out in acidic solutions. ORR and OER reactions are written in Equations (1) and (2).

$$O_2 + 4H^+ + 4e^- \rightarrow 2H_2O \quad (1)$$

$$2H_2O \rightarrow O_2 + 4H^+ + 4e^- \quad (2)$$

The four-electron pathways for ORR were represented by formula 1a-1d

$$* + O_2\ (g) + e^- + H^+ \rightarrow *OOH \quad (1a)$$

$$*OOH + e^- + H^+ \rightarrow H_2O\ (I) + *O \quad (1b)$$

$$*O + e^- H^+ \rightarrow *OH \quad (1c)$$

$$*OH + e^- + H^+ \rightarrow H_2O\ (I) \quad (1d)$$

The four-electron pathways for OER were represented by formula 2a-2d

$$H_2O + * \rightarrow *OH + e^- + H^+ \quad (2a)$$

$$*OH \rightarrow *O + e^- + H^+ \quad (2b)$$

$$H_2O\ (I) + *O \rightarrow *OOH + e^- + H^+ \quad (2c)$$

$$*OOH \rightarrow * + O_2(g) + e^- + H^+ \quad (2d)$$

Here, * denoted the reaction site on the Pt-V_F-Ti_2CF_2. The (I) and (g) are the liquid and gas phases, respectively. In addition, the adsorption energy of catalytic reaction intermediates were calculated by following equations:

$$\Delta E_{O^*} = E_{O^*} - E_* - [E_{H_2O} - E_{H_2}] \quad (3)$$

$$\Delta E_{OH^*} = E_{OH^*} - E_* - [E_{H_2O} - 1/2E_{H_2}] \quad (4)$$

$$\Delta E_{OOH^*} = E_{OOH^*} - E_* - [2E_{H_2O} - 3/2E_{H_2}] \quad (5)$$

Where the E_{O^*}, E_{OH^*}, E_{OOH^*} and E_* is the total energy of Pt-V_F-Ti_2CF_2 adsorption O, OH, OOH and without adsorbent. The E_{H_2O} and E_{H_2} are the total energies of free H2O and H2 molecules in gas phases, respectively. The Gibbs free energy ΔE is defined by equation (6):

$$\Delta G = \Delta E + \Delta ZPE - T\Delta S + \Delta G_u + \Delta G_{pH} \quad (6)$$

ΔZPE and ΔS is the zero point energy and the entropy. The ΔZPE could be obtained from the calculation of vibrational frequencies for the adsorbed species. ΔG_u =-neU, where n was the number of electrons transferred and U was the electrode potential. G_{pH} was refer to the corrected free energy of the H+ ion concentration; the pH was assumed to be zero for the acid media. As for the gas phase molecules, the ZPE can obtain form the NIST database. The free energy of ($H^+ + e^-$) can be replace by $1/2H_2$. The Gibbs free energy of O_2 is calculated by:

$$G_{O_2} = 2G_{H_2O} + 2G_{H_2} - 4 * 1.23\ (eV) \quad (7)$$

For the ORR and OER, to determine the rate-determining step, the ΔG of each reaction step was calculated. Based on the theory as shown in equation (8) and (9), the overpotential of ORR and OER is obtained.

$$\Delta G_{max}^{ORR} = \max\ \{\Delta G_a, \Delta G_b, \Delta G_c, \Delta G_d\} + 1.23\ V \quad (8)$$

$$\Delta G_{max}^{OER} = \max\ \{-\Delta G_a, -\Delta G_b, -\Delta G_c, -\Delta G_d\} + 1.23\ V \quad (9)$$

The HER reaction pathway is presented by following equation:

$$H^+ + e^- \rightarrow 1/2H_2 \quad (10)$$

The Gibbs free energy of H adsorption on Pt-V_F-Ti_2CF_2

$$\Delta G_H = \Delta E_H + \Delta E_{ZPE} - T\Delta S_H \quad (11)$$

And among them, $\Delta S_H \approx -1/2 S_{H_2}$, $\Delta E_{ZPE} = E_{ZPE}^{nH} - E_{ZPE}^{(n-1)H} - 1/2E_{ZPE}^{H_2}$ and $\Delta E_H = E_{nH^*} - E_{(n-1)H^*} - 1/2E_{H_2}$.

Therefore, $\Delta G_H = \Delta E_H + 0.24\ eV$. The Gibbs free energy of HER is only determined by ΔE_H.

The energy correction of the solvation energy (ΔSol) was defined by the following equations (equation 12-13):

$$\Delta Sol = E_{sol} - E_{vac} \quad (12)$$

$$\Delta G_{sol} = \Delta E + \Delta ZPE - T\Delta S + \Delta Sol + \Delta G_u + \Delta G_{pH} \quad (13)$$

Where E_{sol} and E_{vac} is the total energy of the system with and without solvation included,

respectively.

The reason for the poor linear relationship

The linear relationship between ΔG^*_{OH} and ΔG^*_O as well as ΔG^*_{OH} and ΔG_{*OOH} are $\Delta G^*_O=2.43\Delta G^*_{OH}+0.87$ and $\Delta G_{*OOH}=0.7\Delta G_{*OH}+3.42$, and with the coefficient of determination $R^2_{*O}=0.61$ and $R^2_{*OOH}=0.80$, respectively. There is poor linear relationship between ΔG^*_{OH} and ΔG^*_O as well as ΔG^*_{OH} and ΔG_{*OOH}. This is mainly due to three reasons: 1), The O atom (OOH) and OH with different electronic structure. 2), The slope of the ΔG^*_{OH} and ΔG^*_O scale lines is close to 2, which means that adsorbed O has a double bond on the surface, and *OH is bonded by a single bond.[1] 3), The OH adsorption on the Pt-V_F-Ti_2CF_2 shows the abnormal *d*-band center phenomenon, but which is not universally suitable for O atom and OOH.[2] Therefore, the above three factors together lead to the linear relationship between ΔG^*_{OH} and ΔG^*_O as well as ΔG^*_{OH} and ΔG_{*OOH} are poor.

H and catalytic intermediates co-adsorption

Herein, for H atom on the catalyst surface, we considered three adsorption sites (top of the Ti, C and F atom), as shown in Fig. S11(a). Compared with the top of the C and Ti atom, the H atom is more conducive to adsorption on top of the F atom. Based on this, the co-adsorption of H atom and catalytic intermediates is considered. According to the different distance between the H atom and the catalytic intermediate (Fig. S11(b)), two different adsorption configurations for H atom on the *O, $*O_2$ and *OOH are investigated, respectively, as shown in Fig. S11(c-i). For the six pre-adsorption configurations, only the H with the pre-adsorption configuration of Fig. S11(g) can co-adsorption on catalysts surface. After optimizing, the H atom will spontaneously adsorb to the catalytic intermediate, as shown in Fig. S11(d-f) and (h-i). Among them, when the H atom pre-adsorption on the *OOH structure, it combines with an O in OOH, and finally forms H_2O molecule, then spontaneously separated from the catalysts surface (Fig. S11(f)and (i)). Under periodic conditions, the distance between neighboring Pt atoms is 7.84 Å, and this doping density is basically the same as the Pt-doped $Mo_2TiC_2T_x$ reported in the experiment.[3]

More importantly, the diffusive of H atoms to the co-adsorption O atom in Fig. S11(g) with greater than 1eV energy barrier, which is more difficult than the diffusion of H atoms in the solvent to *O. During the ORR process, catalytic intermediates tend to bind to H atoms in the solvent.

The clearer introduction of the abnormal *d*-band theoretical model:

Simply put, for the abnormal *d*-band center model, there is a repulsive effect between OH and *d* state of the metal of Pt-V_F-Ti_2CF_2, which causes a long Pt-O bond length (*OH) to have a weak repulsive effect and a short bond length to have a robust repulsive effect. Therefore, for the abnormal *d*-band center model, the *d*-band center with a high energy level has smaller adsorption energy for OH. Specifically, according previous report,[2] E_{ads} consists of electronic (ΔE_{el}) and electrostatic interactions (ΔE_{es}), and the catalytic intermediate has a similar contribution to ΔE_{es} for certain substrates. Different from the ΔE_{es}, ΔE_{el} is further subdivided into the contributions of *sp*-band and *d*-band as shown in the following equation:

$$\Delta E_{el} = E_{sp} + E_d \tag{14}$$

Where the E_{sp} as the parameters. The E_d is composed of covalent mutual attraction caused by hybridization and repulsion caused by reforming orthogonality.

$$E_d \approx -4\left[(1-f)\frac{V_\pi^2}{|\varepsilon_d - \varepsilon_{1\pi}|} + (1+f)S_\pi V_\pi\right] - 2\left[f\frac{V_\sigma^2}{|\varepsilon_d - \varepsilon_{4\sigma^*}|} + fS_\pi V_\pi\right] \tag{15}$$

Here, f is filling and ε_d is the *d*-band center of the metal atoms of the surface. The $\varepsilon_{1\pi}$ and $\varepsilon_{4\sigma^*}$ is the energy levels of the OH after interaction with the substrate. S_π and V_π are the overlap integral and coupling matrix elements, respectively. According to the muffin-tin orbital theory, V_π is expressed as:

$$V_\pi = \eta_{pd\pi}\frac{\hbar^2 r_d^{3/2}}{m d^{7/2}} \tag{16}$$

The $\eta_{pd\pi}$ and $\frac{\hbar^2}{m}$ are constant. r_d can obtain from the solid states table. d is the bond length of

OH formed with Pt atom. The S is calculated by the equation of $S_\pi \approx -\alpha V$. Based on the above model, Xin *et al.* concluded that there is a repulsive effect between OH and the *d* state of the base metal. Therefore, the larger bond length can lead to the smaller repulsive energy by decreasing the $S_\pi V_\pi$. The bond length is proportional to the adsorption energy. It is attributed to the repulsion between the adsorption state and the *d*-state of metal. Our calculation results are consistent with the abnormal *d*-band theoretical model, as shown Fig. 6(a) and Table S3. Moreover, as the reviewer point out that Fig. 6(c) is the total DOS of O, H and Pt atoms of Pt-V_F-Ti_2CF_2. Additionally, according to the comment of reviewer, to show the anti-bonding and bonding states of Pt-O bond in *OH more visually under -14% and 0% strain, we calculated and analyzed the crystal orbital Hamilton population (COHP), and the result is shown in Fig. R3. Under -14% strain, the antibonding state of Pt-O bond in *OH appears to have higher energy than unstrained. This means that the OH can more stronger bond with the Pt-V_F-Ti_2CF_2, which with -14% compressive strain, compared with unstrained t-V_F-Ti_2CF_2.

References

1 A. Kulkarni, S. Siahrostami, A. Patel and J. K. Norskov, *Chem Rev*, 2018, **118**, 2302-2312.

2 H. Xin and S. Linic, *J. Chem. Phys.*, 2010, **132**, 221101.

3 J. Zhang, Y. Zhao, X. Guo, C. Chen, C.-L. Dong, R.-S. Liu, C.-P. Han, Y. Li, Y. Gogotsi and G. Wang, *Nat. Catal.*, 2018, **1**, 985-992.